Journal of Quantitative Spectroscopy & Radiative Transfer 240 (2020) 106678

Contents lists available at ScienceDirect

Journal of Quantitative Spectroscopy & Radiative Transfer

journal homepage: www.elsevier.com/locate/jqsrt

Saturation of photoassociation in NaCs dark magneto-optical trap

Xiaofeng Wang[a], Wenliang Liu[a,b], Jizhou Wu[a,b,*], Vladimir B. Sovkov[a,c], Jie Ma[a,b], Peng Li[a], Liantuan Xiao[a,b], Suotang Jia[a,b]

[a] State Key Laboratory of Quantum Optics and Quantum Optics Devices, Institute of Laser Spectroscopy, College of Physics and Electronic Engineering, Shanxi University, 92 Wucheng Road, Taiyuan 030006, China
[b] Collaborative Innovation Center of Extreme Optics, Shanxi University, 92 Wucheng Road, Taiyuan 030006, China
[c] St. Petersburg State University, 7/9 Universitetskaya Nab., St. Petersburg 199034, Russia

ARTICLE INFO

Article history:
Received 23 June 2019
Revised 26 September 2019
Accepted 26 September 2019
Available online 28 September 2019

Keywords:
Irap loss spectrum
Intensity dependence
Photoassociaiton rate
High resolution

ABSTRACT

We report the production of ultracold heteronuclear NaCs molecules in excited electronic states by photoassociation (PA) of ultracold Na and Cs atoms. The saturation of the photoassociation scattering probability is observed from the dependence of the trap loss probability on the photoassociation laser intensity. Based on the scattering theory, we estimate the saturation intensity of photoassociation, which is deduced by fitting the experimental data to a saturation model.

1. Introduction

Heteronuclear polar molecules have recently attracted enormous attention owing to their ground state having a large electric dipole moment. [1] The long-range anisotropic dipole-dipole interaction in such systems is the basis for a variety of applications including quantum computing, [2] precision measurements, [3] ultracold chemistry, [4] and quantum simulations. [5] The two primary methods for the production of heteronuclear bi-alkali-metal molecules have been magnetoassociation (MA), as in the case of KRb, NaK, NaLi, NaRb and RbCs, [6–12] and photoassociation (PA), as in the case of LiCs, LiRb, KRb, RbCs, LiK, NaCs and YbRb [1,13–18]. PA offers a unique opportunity of studying the longrange interaction between atoms, and provides a wealth of information about molecular structures in the near-dissociation region. The PA spectra of ultracold atoms have provided significant information about the ground-state collision properties [19] between alkali-metal atoms, accurate measurements of the molecular parameters, the PA rate coefficients, and the radiation lifetimes. [20]

The investigation of the dependence of a PA transition on laser intensity is a topic of interest because of its role in understanding the regime of resonant excitation of converting a pair of free atoms into an excited-state molecule and determining the PA rate. The involved dependence of an amplitude of a resonant signal responsible for the population of a rovibrational level can offer a direct and effective indication for a PA rate. In the past decades, several investigations of the PA rate have been performed in various samples. McKenzie et al. [21] measured the PA spectra for various intensities and durations of the light pulse in a sodium Bose–Einstein condensate and obtained the saturation limit of the PA rate coefficient, the line shape, and the shift in resonance. Schloder et al. [22] report heteronmclear photoassocition spectroscopy in a mixture of magneto-optically trapped ^{6}Li and ^{7}Li. Prodan et al. [23] have measured the intensity dependent rate and frequency shift of a photoassociation transition in a quantum degenerate gas of ^{7}Li. Kraft et al. [24] presented studies of strong coupling in single-photon photoassociation of cesium dimmers using an optical dipole trap. Sourav et al. [1] identified several strong PA resonances. They determined the molecule formation rate and the PA rate coefficient. Mickelson et al. [25] investigated the saturation effects in the PA spectrum of ^{86}Sr. As mentioned above, these studies have presented the laser intensity dependences of the PA rate coefficient in various alkali molecules. However, before our present experiment, measurement of the intensity dependence of the PA of NaCs molecules in the $c^3\Sigma^+$ state for different rotational levels in a vibrational state had not been performed.

In order to understand the regime of strong coupling in PA, which is of pivotal role in the formation of ground state molecules, we report in this paper researches of saturation effects in the PA formation from the Na-Cs continuum to excited molecular states. Using a modulation spectroscopy technique [26], we are able to

* Corresponding Author.
E-mail addresses: wujz@sxu.edu.cn (J. Wu), mj@sxu.edu.cn (J. Ma).

https://doi.org/10.1016/j.jqsrt.2019.106678
0022-4073/

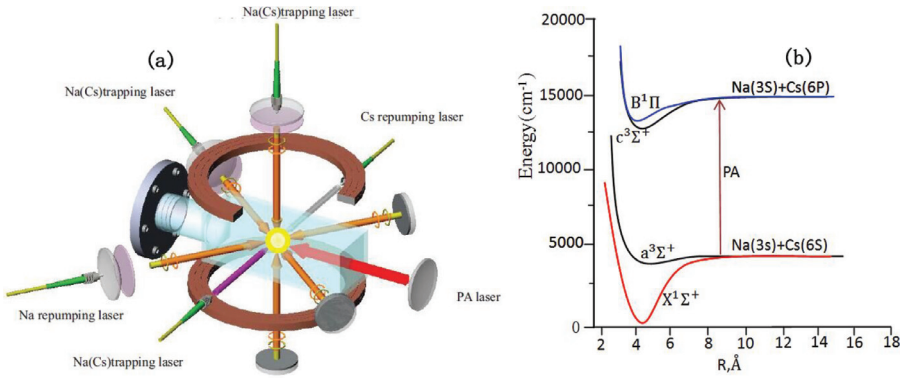

Fig. 1. (a) Experiment setup: Simplified diagram of key elements of the apparatus. The Na and Cs ultracold atom samples are trapped in a dual-species Magneto-Optical Trap (MOT). (b) Potential energy curves(PEC) of the molecule NaCs.

develop systematic investigations of the dependence of the PA rate of polar molecules on the photoassociation laser intensity. Some hyperfine structures of high-lying vibrational levels are observed and analysed in the $c^3\Sigma^+$ electronic state [27]. We investigate the intensity dependence of PA loss rate of PA transitions for different rotational levels at the $v = 61, 64$ vibrational levels of the NaCs $c^3\Sigma^+$ molecular state. PA loss rate exhibits the theoretically predicted dependence on the laser intensity characteristic for the saturation phenomena and the saturation of the PA is observed in our experiment.

2. Experimental setup

Our experiment begins with overlapping dark-spot magneto-optical traps (dark-spot MOTs) of sodium and caesium. The dark-spot MOTs allow us to obtain many ultracold atoms with minimal losses caused by light-assisted interspecies collisions [28]. The spatial overlap of the two MOTs is monitored using a pair of CCD cameras placed orthogonal to each other and a good overlap is ensured for our PA experiments. The details of the apparatus are shown schematically in Fig. 1. Potential energy curves(PEC), which selected low electronic states are also presented. The ^{133}Cs dark-spot MOT typically contains $N_{Cs} \approx 6 \times 10^7$ of Cs atoms at a density of 1.5×10^9 cm^{-3}, with most of the ^{133}Cs atoms in the lower hyperfine ($F = 3$) levels of the $6s^2S_{1/2}$ state. The ^{23}Na dark-spot MOT typically contains $N_{Na} \approx 9 \times 10^6$ of Na atoms at a density of 2.0×10^9 cm^{-3}, with most of the Na atoms in the ~120 μK and ~150 μK respectively, by using a time-of-flight method.

The PA light is served by a widely tuneable continuous-wave Ti:sapphire laser system (Coherent MBR 110, power ~3.5 W, linewidth ~100 KHz). The long-time frequency drift is suppressed within 500 KHz by locking to its self-reference cavity. The absolute frequency of the PA laser is measured by a wavelength meter (High Finesse-Angstrom WS/U) with an accuracy of 30 MHz. The wavelength meter is repeatedly calibrated with the Cs atomic hyperfine resonance transition $6S_{1/2}(F = 4) \rightarrow 6P_{3/2}(F = 5)$ corresponding to the wave number of 11732.176 cm^{-1}. The PA laser beam is collimated to a $1/e^2$ diameter of 0.78 mm with a maximum available average intensity of ~650 W/cm^2.

PA resonances lead to the formation of the excited NaCs molecules, which either spontaneously decay to NaCs molecules in the ground electronic state or to free Na and Cs atoms with high kinetic energies. One of the simplest techniques for detecting a PA transition is to monitor the number of atoms remaining in an MOT. Both mechanisms result in loss of the Na and Cs atoms from the MOT, leading to a decrease in the MOT fluorescence. The formation of the NaCs molecules can thus be detected from this so-called trap loss spectrum. A convenient way to monitor the number of trapped atoms in an MOT is by observing the level of the fluorescence emitted by the atoms as they are continuously bathed in the near-resonant light which forms the MOT. The variation of the number of atoms with the PA laser frequency gives the spectral information [29]. In our experiments, the fluorescence from the Cs (Na) dark-spot MOTs is collected using a lens and detected by an avalanche photodiode (a photomultiplier) with an 852 nm (589 nm) bandpass filter. Direct fluorescence detection is usually not satisfactory because a noise arising from stray fluorescence nearly submerges the useful signal. The lock-in method, based on modulating the fluorescence of the ultracold atoms, is used to improve the detection sensitivity of the trap loss spectroscopy in our experiment. A modulation frequency of 3.4 KHz (3.2 KHz) for the fluorescence from the trapped Cs (Na) atoms is also used in stabilising the trapping laser frequency. The modulated fluorescence is demodulated with a lock-in amplifier (Stanford Research SR830) and recorded by a computer.

The dependence of the PA rate on the laser intensity is of particular interest since we can determine the timescales of a molecule formation. The rate is predicted to increase in intensity at low intensities, while various mechanisms responsible for the saturation of the rate at high intensities have been proposed [32,34]. We experimentally study the PA resonance below the Na($3S_{1/2}$) + Cs($6P_{3/2}$) asymptote, i.e., near the D_2 line of Cs at 852 nm. Accordingly, the PA laser scanning rate is set to 5 MHz/s so that the PA spectra can be observed with a reasonable resolution.

The losses of the trapped Na atoms, experimentally monitored by detecting the Na atomic fluorescence signal, can represent a real PA for heteronuclear NaCs molecules, whereas the losses of the trapped Cs atoms represent the sum of PAs for heteronuclear (NaCs) and homonuclear (Cs_2) molecules. Moreover, the PA-induced loss of the Cs atomic fluorescence monitored simultaneously with the Na atomic fluorescence in the process of the photoassociation is not distinguishable in our experiments. In our previous work [27], we have obtained clear spectroscopy of the ultracold NaCs molecules, Here we focused on two spectra of different rovibrational levels v = 61, 64, which are red detuned from the $3S_{1/2}$ + $6P_{3/2}$ dissociation limit for ~31.7 cm^{-1} and ~14.8 cm^{-1}, respectively.

We have observed some other rotational levels ($J > 1$) and vibrational states, but the loss ratio of the signal is not satisfactory; most resonance lines are nearly indistinguishable. In order to keep the data relatively complete and organised, we do not report the other resonance lines in this letter.

3. Experimental results and discussion

In the regime of the low laser intensity, the PA rate is proportional to the laser power, as shown by Prodan et al. [30] For the high-intensity regime, a semianalytic model of the PA rate was derived in Bohn and Julienne's report, [31] in which the scattering process in a dressed molecular state picture was treated. The PA rate coefficient G can be written as an averaged product of the relative velocity v_r, the maximal inelastic cross section $\beta = \pi/k^2$ (with k being wavenumber), and the scattering probability $\langle|S|^2\rangle$ as follows:

$$G = \left\langle \beta v_r |S|^2 \right\rangle = \left\langle \frac{\pi}{k^2} v_r |S|^2 \right\rangle. \tag{1}$$

The scattering probability between the free scattering state and a bound molecular state is predicted to have a Lorentzian shape and can be written as:

$$\langle|S|^2\rangle = \frac{\gamma\Gamma}{[E-(\Delta+E_1)]^2 + (\frac{\gamma+\Gamma}{2})^2}. \tag{2}$$

where Γ is the absorption rate stimulated by the PA laser, γ is the spontaneous decay rate of the bound excited state, Δ is the PA laser detuning from the resonance of rovibrational levels, E is the energy difference between the two states, and E_1 is the new energy after a light-induced energy shift.

In the theoretical model of Bohn and Julienne [31] for photoassociation in strong laser fields, the rate Γ of the ultracold atoms PA, which depends on the PA laser intensity I, [32] denotes the coupling between the initial continuum wave function $|\Phi(E_{kin} \to 0)\rangle$ with the final bound state wave function $|\Psi(v)\rangle$, and is expressed as:

$$\Gamma = 2\pi (V_{eg})^2 |\langle\Psi(v)|\Phi\rangle|^2. \tag{3}$$

where V_{eg} is the radiative coupling of the scattering and bound states of the electronic transition, which is proportional to the square root of the laser intensity. Generally, Γ depends on the colliding energy E_{kin}, but, thanks to the relative narrowness of the Maxwellian distribution at ultracold temperatures, this dependence can be neglected in our simplified treatment via substituting its effective averaged value. γ is the spontaneous decay rate, modeling the coupling of the upper state with all the (decaying)channels. It is determined only by the coupling between the bound state wave function Ψ and a virtual final free state wave function Φ_1, and can be expressed as:

$$\gamma = 2\pi |\langle\Psi(v)|V|\Phi_1\rangle|^2. \tag{4}$$

with V being an artificial electronic matrix element between the bound excited state and the ultimate free state.

Summarizing, Γ increases linearly, while γ remains unchanged. When this intensity Γ becomes comparable to the spontaneous emission line width of 12 MHz, the PA transition rate begins to saturate. The saturation intensity I_s is defined by $I/I_s = \Gamma/\gamma$. The excited state wave functions $\Psi(v)$ are different at different rotational levels of the same vibrational state, so there is a consequential difference in I_s. One more contribution to this effect is the dependence of the I_s. As this drop-off occurs on an energy scale comparable to γ, it must be included in any PA line-shape analysis, as has been emphasised.

The inelastic-scattering probability in Eq. (2) possesses the form of a Lorentzian distribution, but in the low-energy regime, both the width Γ and the energy shift E_1 exhibit the intensity dependent variation. The maximum amplitude of the resonant line is achieved with $\Delta = E - E_1$ and equals:

$$\langle|S_{max}|^2\rangle = \frac{4\gamma\Gamma}{(\gamma+\Gamma)^2}. \tag{5}$$

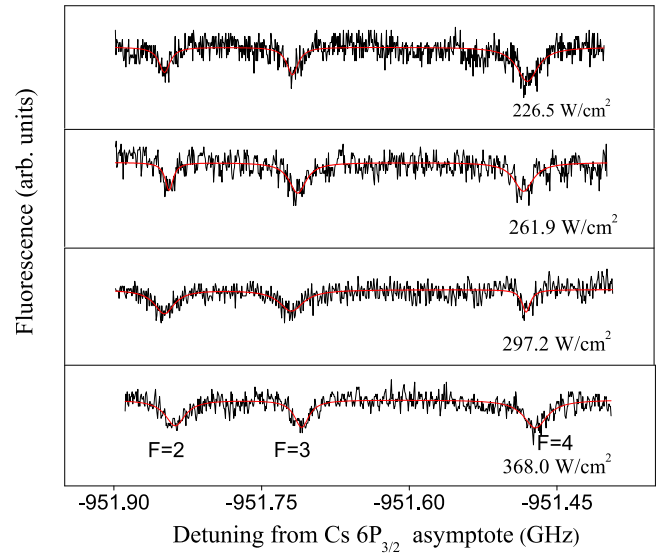

Fig. 2. The high-resolution PA spectra of the v=61 J=1 vibrational state for the $c^3\Sigma^+$ with different intensities. F here is the ordinal number of a hyperfine peak in the entire rovibrational line profile. The NaCs ($3S_{1/2}$ + $6P_{3/2}$) dissociation limit is 11732.176 cm^{-1} [27].

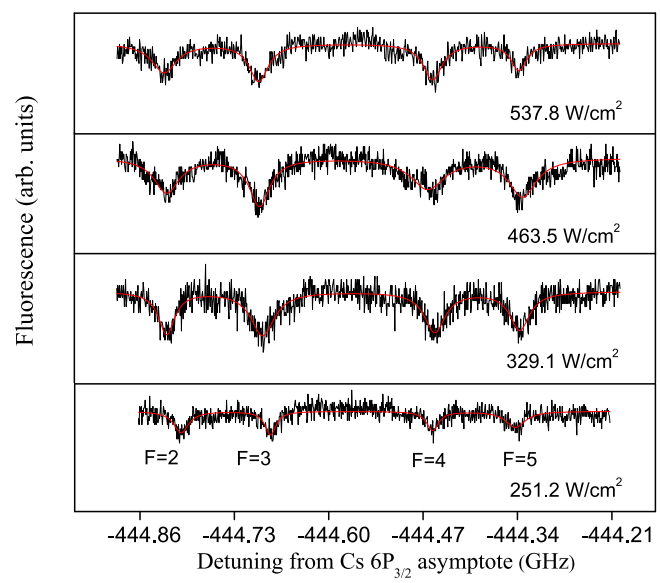

Fig. 3. The high-resolution PA spectra of the v=64 J=1 vibrational state for the $c^3\Sigma^+$ with different intensities. F here is the ordinal number of a hyperfine peak in the entire rovibrational line profile. The NaCs ($3S_{1/2}$ + $6P_{3/2}$) dissociation limit is 11732.176 cm^{-1} [27].

The amplitude Eq. (5) increases proportionally to $\Gamma \sim$I when $\Gamma << \gamma$ and decreases as $1/\Gamma \sim 1/$I when $\Gamma >> \gamma$, having the maximum value at $\Gamma = \gamma$. This behaviour of the amplitude is accompanied by a monotonic increase of the total linewidth $(\Gamma + \gamma)/2$, so that the total integral rate A ($A = 2a\pi I\gamma/(\gamma + aI)$) monotonically increases exhibiting a typical saturation behaviour. Hence, the maxima of the PA loss rate corresponding to the laser intensity I indicate the achievement of the saturation regime $I = I_s$. In order to investigate how and at which intensity the PA rate is saturated, we measured the dependences of the PA probability on the laser intensity for different rotational levels of the v = 61, 64 vibrational states of the $c^3\Sigma^+$ state below the $3S_{1/2}$+ $6P_{3/2}$ dissociation limit. In Figs. 2 and 3, the values of the high-resolution trap-loss for four different laser intensities are shown. The Figs. 2 and 3 show the hyperfine structure that is resolved up to J = 1, v = 61 and J = 1,

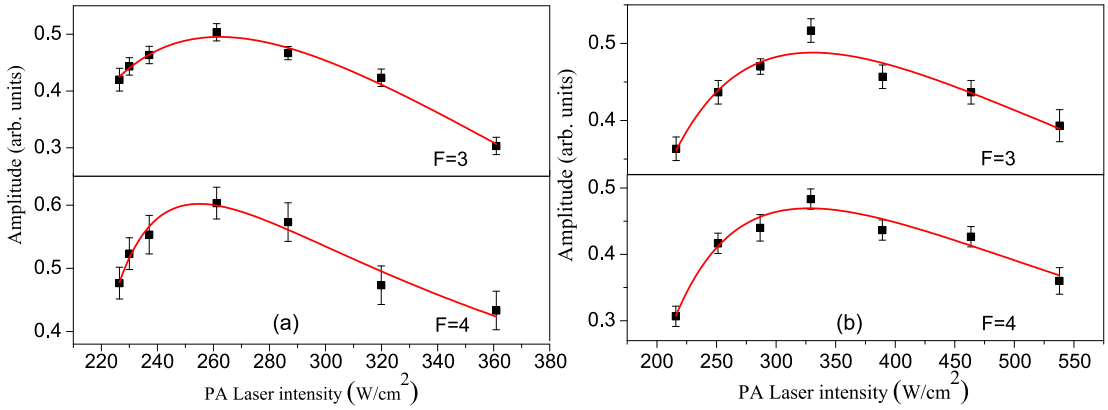

Fig. 4. (a) Plots of the experimental PA loss rate of resonant lines for the v= 61, J= 1, F = 3, 4 hyperfine levels versus the PA laser intensity, with the curves representing the fittings to the saturation model given by Bohn and Julienne [31]. (b) Plots of the PA loss rate of resonant lines for the v= 64, J= 1, F = 3, 4 hyperfine levels versus PA laser intensity, with the curves representing the fittings to the saturation model given by Bohn and Julienne [31].

$v = 64$ with a high signal-to-noise ratio, and that the peak positions remain unchanged. The resonance positions for the two vibrational states $v = 61$ and 64 are 11700.44 cm^{-1}, 11717.36 cm^{-1}, respectively, the assignment of which are in accordance with the results from Ref [33,34].

In Fig. 4, the solid squares denote the experimental data, while the curves represent the fitting to the saturation model of Bohn and Julienne [31,35]. From the figure, we can easily observe that the PA rate increases with the increasing PA intensity at first, and then decreases owing to various mechanisms. When the PA intensity rises to 260 W/cm^2, 250 W/cm^2, 325 W/cm^2, or 330 W/cm^2, depending on the corresponding v and F combinations, the saturation effect is clearly observed. All the rotational progressions can be fitted by formula (5) within experimental accuracies. We only present the results for $v = 61$ $J = 1$, F = 3, 4 and $v = 64$ $J = 1$, F = 3, 4 in the figures, respectively.

4. Conclusion

We have achieved the ultrahigh resolution trap loss spectroscopy by monitoring the fluorescence of trapped sodium atoms as a function of the PA laser frequency. The hyperfine structures of the $c^3\Sigma^+$ state for $v = 61$, J =1, F = 3, 4 and $v = 64$, $J = 1$, F = 3, 4 below the NaCs $3S_{1/2}$ + $6P_{3/2}$ dissociation limit are obtained under different PA laser intensities. The PA loss rate of resonant lines begin to increase and then decrease with PA laser intensities, which the saturation is observed. The PA loss rate are quantitatively in good agreement with the theoretical model. A complete study of the saturation of PA related to rotational levels is required to understand the PA regime of sodium atoms and cesium atoms and to perform the stimulated Raman PA in the well-defined rovibrational levels.

Declaration of competing interest

The authors declared that they have no conflicts of interest to this work.

We declare that we do not have any commercial or associative interest that represents a conflict of interest in connection with the work submitted.

Acknowledgments

This work is supported by the National Key R&D Program of China (grant no. 2017YFA0304203), the National Natural Science Foundation of China (grants nos. 61722507, 61675121, 61705123, 11434007), PCSIRT(no.IRT_17R70), 111 project (grant no. D18001), the Program for the Outstanding Innovative Teams of Higher Learning Institutions of Shanxi (OIT), Fund Program for the Scientific Activities of Selected Returned Overseas Professionals in Shanxi Province, the Fund for Shanxi 1331 Project Key Subjects, the Applied Basic Research Project of Shanxi Province, China (grant no. 201701D221002 and 201801D221004) and collaborative grant by the Russian Foundation for Basic Research and NNSF of China (no. 18-53-53030 in the RFBR classification).

Supplementary material

Supplementary material associated with this article can be found, in the online version, at doi:10.1016/j.jqsrt.2019.106678.

References

[1] Dutta S, Lorenz J, Altaf A, Elliott DS, Chen YP. Phys Rev A 2014;89. 020702(R).
[2] DeMille D. Phys Rev Lett 2002;88:067901.
[3] Hudson ER, Lewandowski HJ, Sawyer BC, Ye J. Phys Rev Lett 2006;96:143004.
[4] Ospelkaus S., Ni K.-K., Wang D., De Miranda M.H.G., Neyenhuis B., Bohn J.L., Jin D.S., Ye J. 2010a. 327, 853
[5] Baranov MA, Dalmonte M, Pupillo G, Zoller P. Chem Rev 2012;112:5012.
[6] Ni K-K, Ospelkaus S, de Miranda MHG, Pe'er A, Neyenhuis B, Zirbel JJ, Kotochigova S, Julienne PS, Jin DS, Ye J. Science 2002;322:231.
[7] Ospelkaus S, Ni K-K, Wang D, de Miranda MHG, Neyenhuis B, Quemener G, Julienne PS, Bohn JL, Jin DS, Ye J. Science 2010;327:853.
[8] Wu C-H, Park JW, Ahmadi P, Will S, Zwierlein MW. Phys Rev Lett 2012;109:085301.
[9] Heo M-S, Wang TT, Christensen CA, Rvachov TM, Cotta DA, Choi J-H, Lee Y-R, Ketterle W. Phys Rev A 2012;86:021602.
[10] Wang FD, He XD, Li XK, Zhu B, Chen J, Wang DJ. New J Phys 2015;17:035003.
[11] Takekoshi T, Reichsollner L, Schindewolf A, Huston JM, Sueur CRL, Dulieu O, Ferlaino F, Grimm R, Nagerl H-C. Phys Rev Lett 2014;113:205301.
[12] Molony PK, Gregory PD, Ji ZH, Lu B, Koppinger MP, Sueur CRL, Blackley CL, Hutson JM, Cornish SL. Phys Rev Lett 2014;113:255301.
[13] Deiglmayr J, Grochola A, Repp M, Mörtlbauer K, Glück C, Lange J, Dulieu O, Wester R, Weidemüller M. Phys Rev Lett 2008;101:133004.
[14] Wang D, Qi J, Stone MF, Nikolayeva O, Wang H, Hattaway B, Gensemer SD, Gould PL, Eyler EE, stwalley WC. Phys Rev Lett 2004;93:243005.
[15] Kerman AJ, Sage JM, Sainis S, Bergeman T, Demile D. Phys Rev Lett 2004;92:033004.
[16] Ridinger A, Chaudhuri S, Salez T, Fernandes DR, Bouloufa N, Dulier O, Salomon C, Chevy F. Europhys Lett 2011;96:33001.
[17] Zabawa P, Wakim A, Haruza M, Bigelow NP. Phys Rev A 2011;84. 061401(R).
[18] Aikawa K, Akamatsu D, Hayashi M, Oasa K, Kobayashi J, Naidon P, Kishimoto T, Ueda M, Inouye S. Phys Rev Lett 2011;105:203001.
[19] Li YQ, Ma J, Wu JZ, Zhang YC, Zhao YT, Wang LR, Xiao LT, Jia ST. Chin Phys B 2014;113:255301.
[20] Zhang YC, Wu JZ, Li YQ, Ma J, Wang LR, Zhao YT, Xiao LT, Jia ST. Chin Phys B 2011;20:123701.
[21] McKenzie C, Denschlag JH, Haffner H, Browaeys A, Araujo EE, Fatemi FK, Jones KM, Simsarian JE, Choa D, Simonib A, Tiesinga E, Julienne PS, Helmerson K, Lett PD, Rolston SL, Phillips WD. Phys Rev Lett 2002;88:120403.
[22] Schloder U, silber C, Deuschle T, Zimmermann C. Phys Rev A 2002;66. 061403(R).

[23] Prodan ID, Pichler M, Junker M, Hulet RG. Phys Rev Lett 2003;91:080402.
[24] Kraft SD, Mudrich M, Staudt MU, Lange J, Dulieu O, Wester R, Weidemuller M. Phys Rev A 2005;71:013417.
[25] Mickelson PG. "saturation effects in photoassociation spectroscopy of ^{86}Sr". Rice University; 2006. Master thesis. Houston, Texas.
[26] Ma J, Wang LR, Zhao YT, Xiao LT, Jia ST. J Mol Spectrosc 2009;255:106.
[27] Liu WL, Wu JZ, Ma J, Li P, Sovkov VB, Xiao LT, Jia ST. Phys Rev A 2016;94:032518.
[28] Shaffer JP, Chalupczak W, Bigelow NP. Phys Rev A 1999;60:R3365.
[29] Jones KM, Tiesinga E, Lett PD, Julienne PS. Rev Mod Phys 2006;78:483.
[30] Prodan ID, Pichler M, Junker M, Hulet RG, Bohn JL. Phys Rev Lett 2003;91:080402.
[31] Bohn JL, Julienne PS. Phys Rev A 1999;60:414.
[32] Liu WL, Wang XF, Wu JZ, Su XL, Wang S, Sovkov VB, Ma J, Xiao LT, Jia ST. Phys Rev A 2017;96:022504.
[33] Wakim A, Zabawa P, Bigelow NP. Phys Chem Chem Phys 2011;13:18887.
[34] Zabawa PJ. Production of ultracold, absolute vibrational groundstate nacs molecules. Department of Physicsand Astronomy, University of Rochester; 2012. Ph.d. thesis. Rochester, New York.
[35] Bohn JL, Julienne PS. Phys Rev A 1996;54:4637.